

Supplemental Information

New Insights into the Metal-Induced Oxidative Degradation Pathways of Transthyretin

Michael L. Poltash, Mehdi Shirzadeh, Jacob W. McCabe, Zahra Moghadamchargari, Arthur Laganowsky,
and David H. Russell*

Department of Chemistry, Texas A&M University, College Station, Texas 77843

Table of Contents

	Page
Supplementary Methods	S2
Figure S1	S4
Figure S2	S5
Figure S3	S6
Figure S4	S7
Figure S5	S8
Figure S6	S9
References	S10

Instrumentation

The homebuilt IM-Orbitrap instrument has been described in detail previously¹. Briefly, ions are generated via static nano-ESI using glass capillaries pulled in-house. Voltages between 2.0 and 3.0 kV are applied to the solution using a platinum wire inserted into the solution. Generated ions are introduced to the instrument through a heated capillary and can be accelerated by a ring electrode before being focused by an RF ion funnel. Ions exiting the ion funnel are modulated using gate 1, thus approximately 50% of the ions enter the 1.45 m PF DT maintained at a helium pressure of ~1.5 Torr for mobility separation. A second gate (gate 2) is positioned at the exit of the DT, thus approximately 50% of the ions are transmitted to an RF-only octupole ion guide. These ions are then collected and trapped in the higher energy collisional dissociation (HCD) cell of the Orbitrap. Ions trapped in the HCD cell are relaxed and transferred to the C-trap which injects ions into the Orbitrap for mass analysis. Orbitrap settings of 100 ms maximum inject times and resolution of 17,500 were used for all experiments. A schematic of the instrument and the details of operation of the instrument with its implementation as a Fourier transform-IM-MS instrument has been described elsewhere.¹

Surface induced dissociation (SID) experiments were performed on a modified Waters Synapt G2. Samples were also introduced by static nano-ESI with a capillary voltage between ~1.2 and 1.5 kV using the same emitters as described above. Other parameters include: source pressure (5-6 mBar), sampling voltage (20 V), trap flow (2 L/min) and He flow (120 ml/min).

Size-Exclusion Chromatography

Superdex HiLoad 16/600 75 µg column (ÄKTA Explorer, GE Healthcare) was used for size exclusion chromatography. The column was equilibrated and eluted with HEPES (50 mM), NaCl (50 mM), EDTA (10 mM) and DTT (1mM), pH=7.4 at 4 °C.

Data Processing

Raw MS data was acquired using Exactive software and converted using Python scripts making use of *Multiplierz*. Extracted ion chromatograms were subsequently obtained and processed using custom Python scripts. IMS peak fitting was accomplished using Origin with R^2 thresholds > 0.95 .

Chemicals and Materials

TTR was expressed and purified in-house as described previously². Samples were buffer exchanged using centrifugal buffer exchange devices (Micro Bio-Spin 6, Bio-Rad) into 200 mM ammonium acetate before analyses. Copper acetate, zinc acetate, iron acetate, nickel acetate, tris(2-carboxyethyl)phosphine (TCEP), N-ethylmaleimide (NEM), and chromium (VI) ICP standard were purchased from Sigma Aldrich and diluted in 200 mM ammonium acetate. Thyroxine (T_4) was purchased from Alfa Aesar and diluted in DMSO to the final concentration of 40 μ M and mixed in 1 to 10 molar ratio with TTR.

Sequence of TTR

GSGPT GTGES KCPLM VKVLD AVRGS PAINV AVHVF RKAAD DTWEP FASGK TSESG ELHGL TTEEE FVEGI
YKVEI DTKSY WKALG ISPFH EHAEV VFTAN DSGPR RYTIA ALLSP YSYST TAVVT NPKE

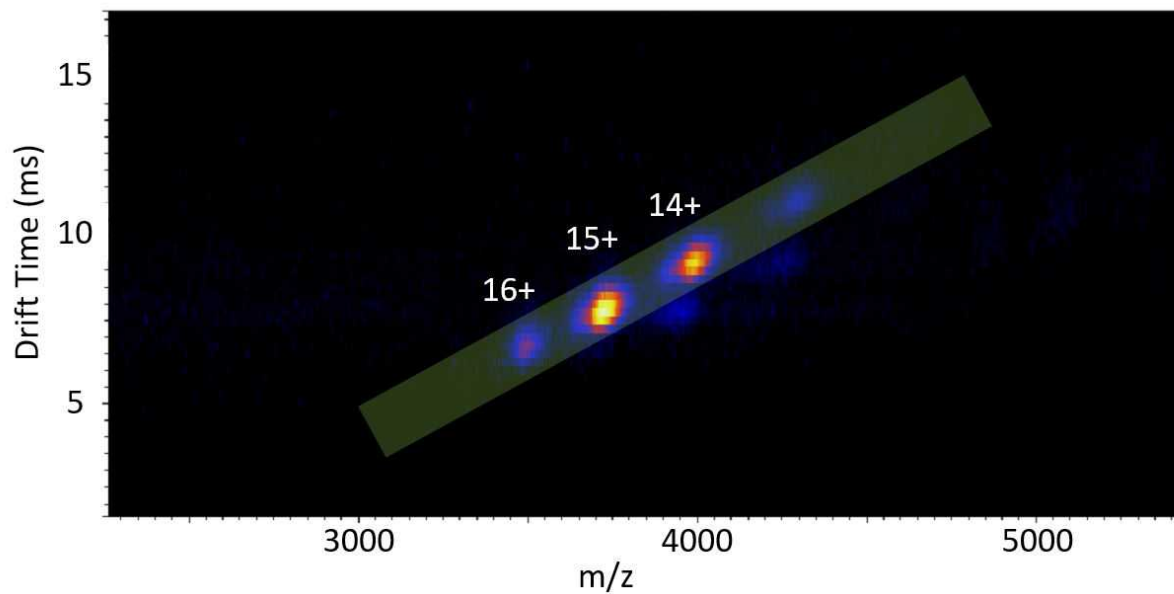


Figure S1. The 2D IM-MS plot of TTR collected using the Waters Synapt G2. $[\text{TTR} + 14\text{H}^+]^{14+}$ and $[\text{TTR} + 15\text{H}^+]^{15+}$ both populate the compact, native conformer of the protein which retains both Zn(II) and oxidation.

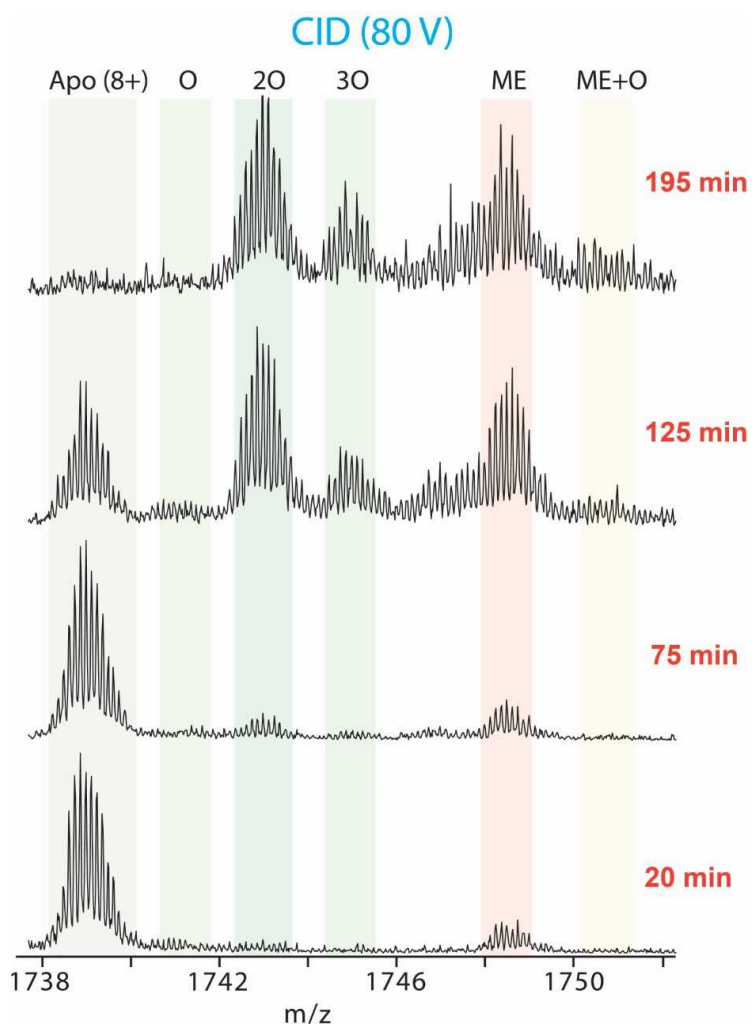


Figure S2. $[\text{TTR} + 8\text{H}^+]^{8+}$ monomer fragment using CID showing the time-dependent oxidation of TTR. CID, however, unfolds the monomer in the gas-phase dissociating the noncovalent Zn(II) interactions observed in SID.

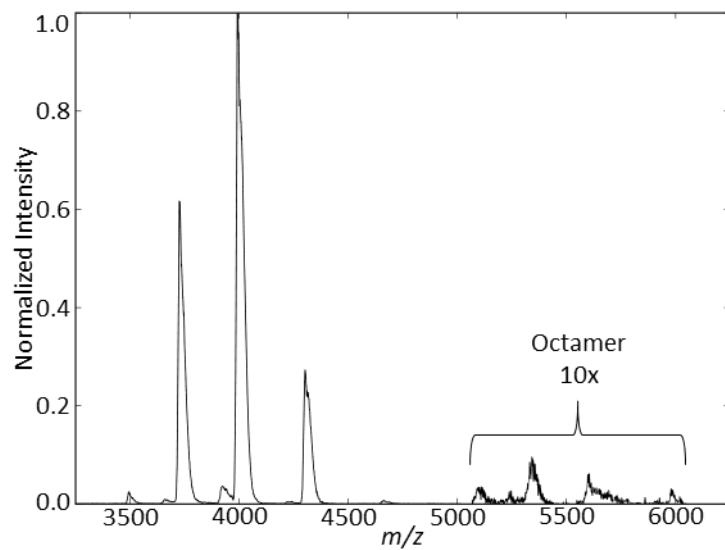


Figure S3. The mass spectrum of TTR after 64 minutes of continuous ESI. Octamer formation occurs simultaneously with Cys-12/Pro-13 backbone fragmentation. Octamer region of the MS is magnified 10x.

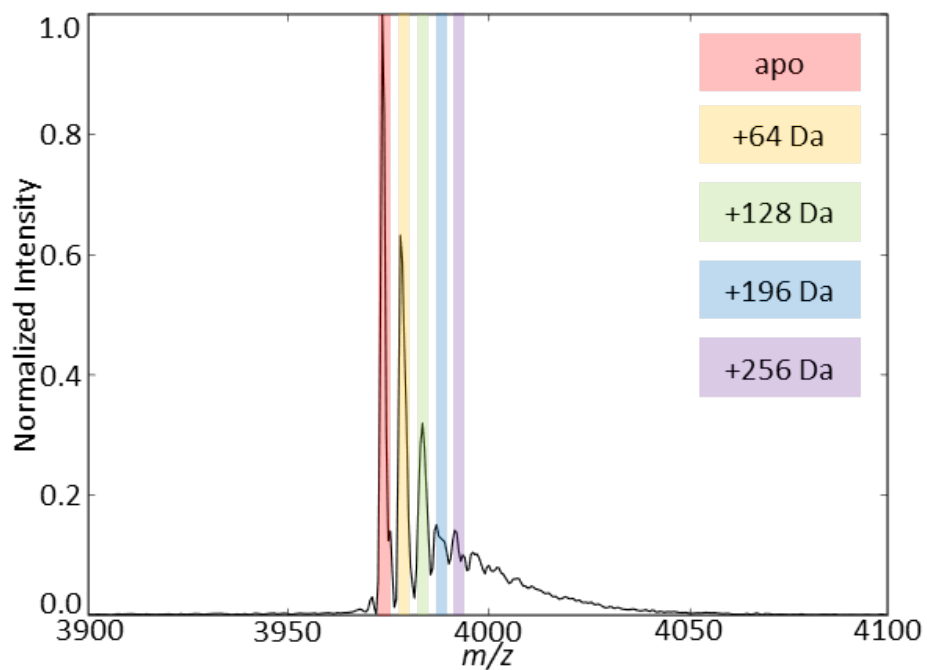


Figure S4. $[\text{TTR} + 14\text{H}^+]^{14+}$ tetramer after 60 minutes of analysis using a gold-coated nano-ESI emitter. Oxidation occurs much more slowly; however, peak broadening is observed attributed to Na^+ adduction over time.

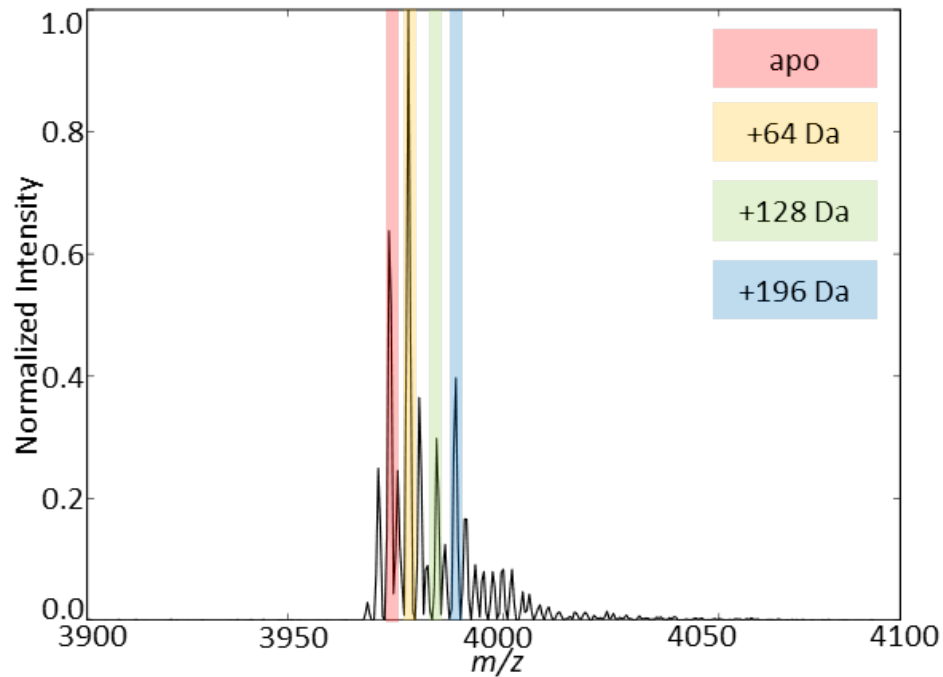


Figure S5. $[TTR + 14H^+]^{14+}$ tetramer after 60 minutes of analysis after size exclusion chromatography in the presence of EDTA to strip metals from solution before analysis. Metal removal resulted slowed oxidation and fragmentation approximately 2-fold. Importantly, EDTA chelates metals most readily at pH > 9 at which point TTR denatures, therefore, optimal conditions for chelation were not attainable without perturbing the structure of TTR.

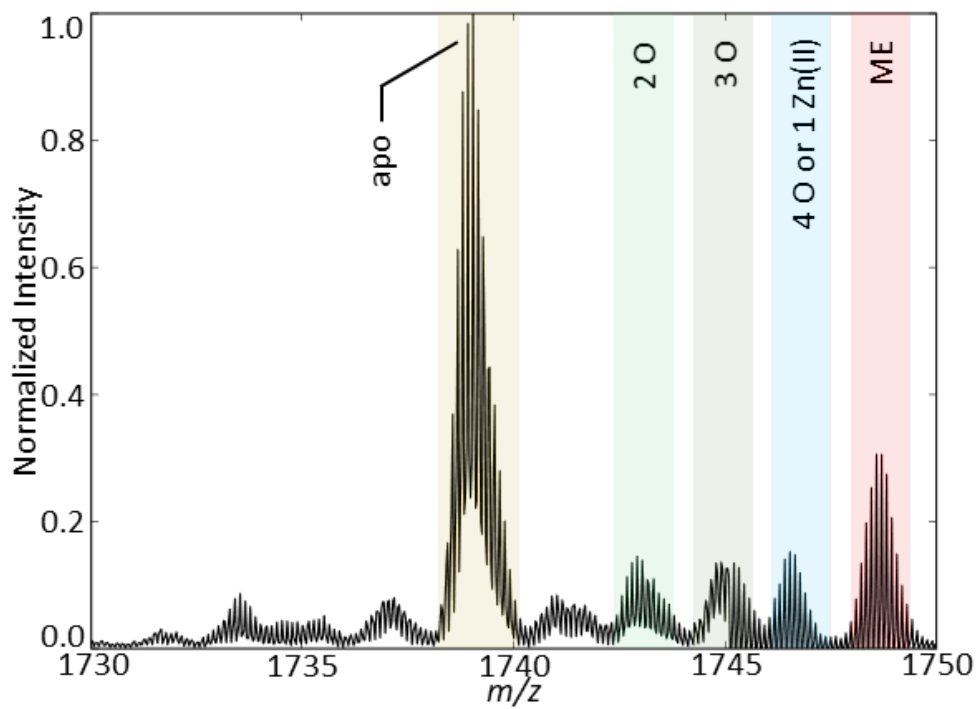


Figure S6. $[\text{TTR} + 8\text{H}^+]^{8+}$ monomer fragment obtained directly after the addition of equimolar CuCH_3OOH . Addition of $\text{Cu}(\text{II})$ in solution immediately induces oxidation without the need for an applied potential.

References

1. Poltash, M. L.; McCabe, J. W.; Shirzadeh, M.; Laganowsky, A.; Clowers, B. H.; Russell, D. H., Fourier Transform-Ion Mobility-Orbitrap Mass Spectrometer: A Next-Generation Instrument for Native Mass Spectrometry. *Analytical Chemistry* **2018**, *90* (17), 10472-10478.
2. Shirzadeh, M.; Boone, C. D.; Laganowsky, A.; Russell, D. H., Topological Analysis of Transthyretin Disassembly Mechanism: Surface-Induced Dissociation Reveals Hidden Reaction Pathways. *Analytical Chemistry* **2019**, *91* (3), 2345-2351.